Published in final edited form as:
Int J Radiat Oncol Biol Phys. 2008 April 1; 70(5): 1397–1402. doi:10.1016/j.ijrobp.2007.08.052.

^{18}F-FLUORODEOXYGLUCOSE POSITRON EMISSION TOMOGRAPHY-BASED ASSESSMENT OF LOCAL FAILURE PATTERNS IN NON–SMALL-CELL LUNG CANCER TREATED WITH DEFINITIVE RADIOTHERAPY

Sonal Sura, M.D.[*], **Carlo Greco, M.D.**[*], **Daphna Gelblum, M.D.**[*], **Ellen D. Yorke, Ph.D.**[†], **Andrew Jackson, Ph.D.**[†], and **Kenneth E. Rosenzweig, M.D.**[*]

[*] Department of Radiation Oncology, Memorial Sloan-Kettering Cancer Center, New York, NY

[†] Department of Medical Physics, Memorial Sloan-Kettering Cancer Center, New York, NY

Abstract

Purpose—To assess the pattern of local failure using ^{18}F-fluorodeoxyglucose (FDG)-positron emission tomography (PET) scans after radiotherapy (RT) in non–small-cell lung cancer (NSCLC) patients treated with definitive RT whose gross tumor volumes (GTVs) were defined with the aid of pre-RT PET data.

Method and Materials—The data from 26 patients treated with involved-field RT who had local failure and a post-RT PET scan were analyzed. The patterns of failure were visually scored and defined as follows: *(1)* within the GTV/planning target volume (PTV); *(2)* within the GTV, PTV, and outward; (3) within the PTV and outward; and *(4)* outside the PTV. Local failure was also evaluated as originating from nodal areas vs. the primary tumor.

Results—We analyzed 34 lesions. All 26 patients had recurrence originating from their primary tumor. Of the 34 lesions, 8 (24%) were in nodal areas, 5 of which (63%) were marginal or geographic misses compared with only 1 (4%) of the 26 primary recurrences ($p = 0.001$). Of the eight primary tumors that had received a dose of <60 Gy, six (75%) had failure within the GTVand two (25%) at the GTV margin. At doses of ≥60 Gy, 6 (33%) of 18 had failure within the GTV and 11 (61%) at the GTV margin, and 1 (6%) was a marginal miss ($p < 0.05$).

Conclusion—At lower doses, the pattern of recurrences was mostly within the GTV, suggesting that the dose might have been a factor for tumor control. At greater doses, the treatment failures were mostly at the margin of the GTV. This suggests that visual incorporation of PET data for GTV delineation might be inadequate, and more sophisticated approaches of PET registration should be evaluated.

Keywords

Non–small-cell lung cancer; FDG-PET scan; Local failure; Definitive radiotherapy

Reprint requests to: Kenneth E. Rosenzweig, M.D., Department of Radiation Oncology, Memorial Sloan-Kettering Cancer Center, 1275 York Ave., New York, NY 10021. Tel: (212) 639-6025; Fax: (212) 639-2417; rosenzwk@mskcc.org.

Conflict of interest: none.

INTRODUCTION

Lung cancer remains the leading cause of death from cancer in both men and women in the United States (1). For inoperable non–small-cell lung cancer (NSCLC) managed by radiotherapy (RT) alone or combined chemoradiotherapy, local failure remains a major challenge. The probability of local tumor control increases with greater applied radiation doses (2,3); however, to keep the risk of radiation-induced side effects low, it is necessary to reduce the treatment volumes as much as possible (4). To achieve this, many centers only treat the gross tumor and omit the elective nodal regions (5). More recently, high-precision image-guided RT has been used as a technique for dose acceleration with the aim of reducing setup uncertainties and detecting organ motion while maintaining smaller target volumes (6).

With recent advances in targeted RT delivery and the promotion of involved-field RT, accurate staging and target delineation is important. Interphysician variability in target volume delineation has been found to be a great source of inconsistency in treatment planning for NSCLC (7,8). ^{18}F-fluorodeoxyglucose positron emission tomography (^{18}FDG-PET) has been used as a method to improve the accuracy of target delineation and has been shown to reduce interobserver variability in NSCLC (9–12).

The issues of accurate tumor edge definition and tumor motion effects are well established, and unresolved concerns exist about using ^{18}FDG-PET for NSCLC staging and gross tumor volume (GTV) delineation (13–15). Information from ^{18}FDG-PET scans can lead to altered staging and target volumes either by upstaging, because of previously undetected nodal disease, or downstaging, because of atelectasis or previously suspicious nodal disease found to be metabolically insignificant (8,9,16–20). The effect of pre-RT ^{18}FDG-PET data incorporation into treatment planning on the patterns of local failure has been insufficiently investigated. The effect of ^{18}FDG-PET–based mediastinal volume assessment using visual fusion has recently been reported by two studies (21,22), which indicated very low rates of nodal failures in patients selectively irradiated to the areas of FDG avidity in the mediastinum.

The knowledge and understanding of the post-RT patterns of failure is still fairly limited when assessed by computed tomography (CT), whose accuracy can be impaired by radiation-induced fibrosis, which is difficult to differentiate from viable tumor tissue (23). The use of metabolic information from the post-RT ^{18}FDG-PET scan might overcome this limitation and better define the spatial relationships between the targeted volume and the recurrence site (24).

The aim of the present analysis, therefore, was to investigate the relationships among the pre-RT ^{18}FDG-PET–defined target volumes, prescription dose, and post-RT ^{18}FDG-PET–based patterns of failures for the primary tumor and involved nodal areas in inoperable NSCLC (Fig. 1).

METHODS AND MATERIALS

Between 2001 and 2005, a total of 230 patients with Stage I–IIIB NSCLC were treated with involved-field RT to doses of 50–90 Gy at Memorial Sloan-Kettering Cancer Center. At treatment planning, all patients underwent a planning CT scan (Model PQ 5000 AcQSim, Marconi/Philips Medical Systems, Cleveland, OH) while immobilized in the treatment position, supine, with their arms raised in a customized alpha-cradle mold (Alpha Cradle Molds, Akron, OH). The GTV consisted of all known sites of disease defined by CT with the visual aid of ^{18}FDG-PET scan data, without inclusion of the elective nodal targets. The planning target volume (PTV) was determined from the GTV, with an automatic expansion of 10–18 mm that could be edited in a patient-specific fashion. Although treatment was delivered without respiratory gating, the physiologic motion was accounted for at the discretion of the treating physician and was considered when adding the margin to the GTV. Critical normal

structures were also contoured. Treatment planning was performed with the Memorial Sloan-Kettering Cancer Center treatment planning system, which has previously been described (25–28). Tissue inhomogeneity corrections were applied to all dose calculations (25). All patients were treated with conventional fractionation (1.8–2.0 Gy) with no planned treatment breaks. The prescription dose varied depending on the tumor shape, size, and location and patients' ability to tolerate RT.

Of the 230 patients, 82 had local failure. Of these 82 patients, 26 had an in-house post-RT PET–CT scan that could be registered electronically with the treatment planning CT scan; this subgroup was the patient population for the present analysis. The remaining 56 patients with local failure either did not undergo FDG-PET after development of the local failure or had undergone FDG-PET at an outside institution that could not be registered with our planning system. The initial planning scan, all related contours, and the original treatment plan were restored from the archives and the post-RT PET study was also imported into the planning system. Registration with in-house software was done using the bony anatomy as visualized on the planning scan and post-RT attenuation scan (CT-to-CT registration). Using the Memorial Sloan-Kettering Cancer Center planning system, the post-RT PET–based recurrences were contoured using a fixed threshold of 42% of the maximum standardized uptake value (13).

Positron emission tomography scans can be difficult to interpret after RT owing to increases in standardized uptake value uptake as a result of radiation-induced inflammation (29). The failures were defined visually and independently by three radiation oncologists and were characterized as follows: *(1)* entirely within the GTV/PTV; *(2)* within the GTV/PTV and extending outward; *(3)* within the PTV but not the GTV and extending outward (marginal miss); and *(4)* outside, but within 1 cm, of the PTV (geographic miss; Fig. 2). The volume of recurrence overlap with the PTV was also calculated to objectively confirm the results. After re-examining the CT and FDG-PET scans of the 26 patients with evidence of local failure, the failures were assessed as originating from the primary tumor site vs. the nodal areas. Dose–volume histograms were generated for each recurrence, the PTV, and the volume of overlap between the PTV and the recurrence. The dose received by 95% (D_{95}) of each overlap region was recorded. A dose level of 60 Gy was selected to differentiate between low- and high-dose treatment to assess the effect of dose on the recurrence pattern.

Statistical analysis was done using the Kaplan-Meier (30) and chi-square methods, and all times were calculated from the initiation of chemotherapy or RT.

RESULTS

We analyzed the data from 26 patients with 34 lesions. The patient characteristics are detailed in Table 1. The prescription dose was 50–90 Gy (median, 72 Gy). Seven patients (27%) were treated using intensity-modulated RT. Cisplatin-based chemotherapy was used in 14 patients, 8 of whom underwent sequential chemotherapy and 6 of whom received concurrent chemoradiotherapy. The median follow-up time was 20 months, with a median time to local failure of 13 months. The 2-year overall survival rate was 59%, with a median survival time of 26 months.

Outcome

The local recurrences were scored using the four definitions listed in the "Methods and Materials" section (Table 2). Interobserver variability among the three physicians was minimal (1 of 34), suggesting that despite the limitations of PET scan imaging after RT, the scans were consistently interpreted. All 26 patients developed a recurrence arising from the primary tumor; the eight remaining lesions were in nodal areas. Of the eight nodal recurrences, five (63%)

were marginal or geographic misses compared with only one (4%) of the 26 primary recurrences were of the same failure pattern ($p = 0.0001$).

The dose of 60 Gy, which is still standard in the treatment of inoperable NSCLC, was used to examine the relationship between the radiation dose and pattern of failure. In the 26 recurrences arising within the primary tumor, of the 8 patients treated with <60 Gy, 6 (75%) had treatment failure completely within the GTV and PTV and 2 (25%) within the GTV, PTV, and extending outward. When the prescription dose to the PTV was ≥60 Gy (n = 18), the observed failure patterns for the primary tumors changed, with only 6 (33%) of 18 contained within the GTV and PTV, 11 (61%) within the GTV and PTV and extending outward, and 1 (6%) within the PTV and extending outward (marginal miss; $p < 0.05$).

A dose–volume histogram analysis was also performed to objectively evaluate the dose distribution within the regions of interest. When a recurrence developed in the primary tumor, the D_{95} for the region of overlap was sufficiently close to the prescription dose that the patients with a prescription dose >60 Gy were identical to those whose overlap D_{95} was >60 Gy, indicating that no large cold spots were present within the region of overlap. As a consequence, the failure patterns determined by prescription dose and those deter-mined by the D_{95} were identical (Table 3).

DISCUSSION

The purpose of this study was to contribute to the limited knowledge of patterns of failure in inoperable NSCLC after definitive RT. Using post-RT FDG-PET data to define recurrence, this analysis showed that even when visual incorporation of pre-RT ^{18}FDG-PET data were used for treatment planning, the local failure rates were high. The patterns of recurrence differed depending on the whether the site of failure was in the primary tumor or in the nodal regions. All patients in this study developed recurrence at the primary tumor site; however, the pattern of failure was dependent on the radiation dose. Not surprisingly, at low doses (<60 Gy) most recurrences were within the target volume (GTV/PTV), likely reflecting an insufficient dose for tumor control. At greater doses (≥60 Gy), the recurrences occurred mostly at the margin of the target volume (PTV and outward), suggesting inadequate target delineation, insufficient GTV to PTV expansion, and/or the need for tumor motion control. The patterns of failure in the nodal recurrences were mainly marginal or geographic misses, suggesting poor volume delineation with suboptimal appreciation of microscopically involved nodal disease at treatment planning.

The use of ^{18}FDG-PET/CT has become a part of the standard of care for the staging of NSCLC (31). Recently, PET/CT has been used as a tool to enhance the accuracy of target volume delineation. PET and CT information can be incorporated into the treatment planning in three different ways: visual fusion, software fusion, and hardware fusion. In visual fusion, the two imaging modalities are simply compared side by side. In software fusion, the CT and PET images from two separate studies are electronically registered with each other using a variety of anatomic features, and the images corresponding to the same anatomic site are overlaid or viewed side-by-side with specialized software. Hardware fusion is obtained from PET/CT scanners, in which the two image sets are acquired during the same session, self-registered (given patient compliance), and can be viewed separately or overlaid.

Several studies have shown that the incorporation of PET data leads to changes in the target volume compared with delineation with CT alone. Kiffer *et al.* (17) have shown that if coronal thoracic PET images were viewed at RT planning, the anteroposterior volumes changed in 26.7% of cases. Using software fusion, Munley *et al.* (32) reported an increase in target volume in 34% of cases compared with CT-defined volumes. Erdi *et al.* (18) performed a study in

which the patients' CT and PET images were fused using software. They found a change in the PTV definition in all patients, with 7 who had an increase in PTV owing to the inclusion of FDG-avid lymph nodes not seen on CT and 4 who had a reduction in the PTV because of exclusion of atelectatic lung. To date, few studies with hardware fusion (integrated PET/CT devices) have been conducted. Ciernik *et al.* (11) used hardware-fused images in treatment planning and observed significant changes (≥25%) in the GTVs in 5 of 6 lung cancer patients. In a prospective study, Ashamalla *et al.* (10) integrated co-registered PET/CT images for 19 patients. A clinically significant (≥25%) treatment volume modification was observed in 52% of the cases, with a consequent change in the PTV of >20% in 42% of patients.

The information gathered from the FDG-PET data could have a different effect on target delineation for primary tumors vs. nodal regions. To date, the addition of PET data in the delineation of the primary tumor, compared with CT data alone, has shown limited value, given the high resolution of CT and the relatively low resolution of current PET scanners. However, in some cases, the CT-delineated GTV includes CT abnormalities that appear totally devoid of FDG activity and can safely be excluded from the GTV, resulting in a significant reduction of the target volume (33).

The situation for nodal target regions is different. Because routine elective nodal RT is often omitted in NSCLC, accurate determination of the involved nodal areas is crucial in modern treatment planning (34). ^{18}FDG-PET alone has been considered to be superior to CT in mediastinal staging, and, recently, the diagnostic power of integrated PET/CT has been shown to be greater than either CT or PET alone (30).

Many studies have shown significant changes in GTV with the inclusion or exclusion of PET-defined nodal areas compared with the CT-generated GTV (35,36). De Ruysscher *et al.* (21), in a prospective clinical study, evaluated the recurrence pattern after visually fused ^{18}FDG-PET data for selective mediastinal node irradiation in 44 patients with NSCLC. Only one nodal recurrence was reported with mediastinal FDG uptake. Such a low nodal failure rate can be explained by "unintended" elective irradiation. This hypothesis has been corroborated by the finding of a very low nodal failure rate recently reported by Belderbos *et al.* (22) in a dose-escalation trial of involved-field irradiation in ^{18}FDG-PET staged patients. However, in the present series, 8 (24%) of the 34 recurrences were in nodal areas and were mostly classified as marginal or geographic misses. The visual incorporation of the ^{18}FDG-PET data at treatment planning might have been inadequate in determining the extent of lymph node involvement.

The efficacy of local RT is greatly predicted on our ability to accurately define the target volume, thereby reducing the risk of a geographic miss and, ultimately, translating to better local control and improved survival. In NSCLC patients treated with definitive RT, dose escalation is often hindered by an excessive dose to critical tissues, particularly the normal lung and the spinal cord. Therefore, techniques such as intensity-modulated RT and image-guided RT are being implemented to reduce the dose to normal tissue while targeting the tumor (6,37). These technologies require accurate staging and target definition to be effective.

CONCLUSION

This study is the first to report on the clinical results and effects of the use of visual fusion of FDG-PET and CT data at treatment planning. Despite existing studies on the use of PET data for NSCLC supporting a significant advantage in accurate target volume delineation at treatment planning, the results of the present analysis suggest that potential difficulties in target definition remain, especially with regard to the nodal volumes. One possible explanation is that visual fusion of PET images to CT images might be insufficient for accurate detection of nodal disease, as well as cause anatomic displacement. Therefore, more sophisticated

approaches of image registration should be evaluated to further enhance the use of ^{18}FDG-PET in target definition for RT for NSCLC.

References

1. Jemal A, Siegel R, Ward E, et al. Cancer statistics, 2006. CA Cancer J Clin 2006;56:106–130. [PubMed: 16514137]
2. Willner J, Baier K, Caragiani E, et al. Dose, volume, and tumor control predictions in primary radiotherapy of non–small-cell lung cancer. Int J Radiat Oncol Biol Phys 2002;52:382–389. [PubMed: 11872283]
3. Rengan R, Rosenzweig KE, Venkatraman E. Improved local control with higher doses of radiation in large-volume stage III non–small-cell lung cancer. Int J Radiat Oncol Biol Phys 2004;60:741–747. [PubMed: 15465190]
4. Nelson C, Starkschall G, Chang JY. The potential for dose escalation in lung cancer as a result of systematically reducing margins used to generate planning target volume. Int J Radiat Oncol Biol Phys 2006;65:573–586. [PubMed: 16690439]
5. Rosenzweig KE, Sim SE, Mychalczak B, et al. Elective nodal irradiation in the treatment of non–small-cell lung cancer with three-dimensional conformal radiation therapy. Int J Radiat Oncol Biol Phys 2001;50:681–685. [PubMed: 11395236]
6. Onimaru R, Shirato H, Shimizu S, et al. Tolerance of organs at risk in small-volume, hypofractionated, image-guided radiotherapy for primary and metastatic lung cancers. Int J Radiat Oncol Biol Phys 2003;56:126–135. [PubMed: 12694831]
7. Senan S, Chapet O, Lagerwaard FJ, et al. Defining target volumes for non-small cell lung carcinoma. Semin Radiat Oncol 2004;14:308–314. [PubMed: 15558505]
8. Giraud P, Grahek D, Montravers F, et al. CT and (18)F-deoxyglucose (FDG) image fusion for optimization of conformal radiotherapy of lung cancers. Int J Radiat Oncol Biol Phys 2001;49:1249–1257. [PubMed: 11286831]
9. Mah K, Caldwell CB, Ung YC, et al. The impact of (18)FDG-PET on target and critical organs in CT-based treatment planning of patients with poorly defined non–small-cell lung carcinoma: A prospective study. Int J Radiat Oncol Biol Phys 2002;52:339–350. [PubMed: 11872279]
10. Ashamalla H, Rafla S, Parikh K, et al. The contribution of integrated PET/CT to the evolving definition of treatment volumes in radiation treatment planning in lung cancer. Int J Radiat Oncol Biol Phys 2005;63:1016–1023. [PubMed: 15979817]
11. Ciernik IF, Dizendorf E, Baumert BG, et al. Radiation treatment planning with an integrated positron emission and computer tomography (PET/CT): A feasibility study. Int J Radiat Oncol Biol Phys 2003;57:853–863. [PubMed: 14529793]
12. Fox JL, Rengan R, O'Meara W, et al. Does registration of PET and planning CT images decrease interobserver and intra-observer variation in delineating tumor volumes for non–small-cell lung cancer? Int J Radiat Oncol Biol Phys 2005;62:70–75. [PubMed: 15850904]
13. Erdi YE, Mawlawi O, Larson SM, et al. Segmentation of lung lesion volume by adaptive positron emission tomography image thresholding. Cancer 1997;80:2505–2509. [PubMed: 9406703]
14. Stevens CW, Munden RF, Forster KM, et al. Respiratory-driven lung tumor motion is independent of tumor size, tumor location and pulmonary function. Int J Radiat Oncol Biol Phys 2001;51:62–68. [PubMed: 11516852]
15. Wong JW, Sharpe MB, Jaffray B, et al. The use of active breathing control (ABC) to reduce margin for breathing motion. Int J Radiat Oncol Biol Phys 1999;44:911–919. [PubMed: 10386650]
16. MacManus MP, Hicks RJ, Ball DA, et al. ^{18}Fluoro-2-deoxyglu-cose positron emission tomography staging in radical radiotherapy candidates with non-small cell lung cancer. Cancer 2001;92:886–895. [PubMed: 11550162]
17. Kiffer JD, Berlangieri SU, Scott AM, et al. The contribution of ^{18}fluoro-2-deoxyglucose positron emission tomographic imaging to radiotherapy planning in lung cancer. Lung Cancer 1998;19:167–177. [PubMed: 9631364]

18. Erdi YE, Rosenzweig KE, Erdi AK, et al. Radiotherapy treatment planning for patients with non-small cell lung cancer using positron emission tomography (PET). Radiother Oncol 2002;62:51–60. [PubMed: 11830312]
19. Bradley J, Thorstad W, Mutic S, et al. Impact of FDG-PET on radiation therapy volume delineation in non–small-cell lung cancer. Int J Radiat Oncol Biol Phys 2004;59:78–86. [PubMed: 15093902]
20. Greco C, Rosenzweig KE, Cascini G, et al. Current status of PET/CT for tumour volume definition in radiotherapy treatment-planning for non small cell lung cancer (NSCLC). Lung Cancer 2007;57:125–135. [PubMed: 17478008]
21. De Ruysscher D, Wanders S, Van HE, et al. Selective mediastinal node irradiation based on FDG-PET scan data in patients with non–small-cell lung cancer: A prospective clinical study. Int J Radiat Oncol Biol Phys 2005;62:988–994. [PubMed: 15989999]
22. Belderbos JS, Heemsbergen WD, De JK, et al. Final results of a phase I/II dose escalation trial in non–small-cell lung cancer using three-dimensional conformal radiotherapy. Int J Radiat Oncol Biol Phys 2006;66:126–134. [PubMed: 16904518]
23. Erasmus JJ, Gladish GW, Broemeling L, et al. Interobserver and intraobserver variability in measurement of non–small-cell lung carcinoma lung lesions: Implications for assessment of tumor response. J Clin Oncol 2003;21:2575–2582.
24. MacManus MP, Hicks RJ, Mathews JP, et al. Positron emission tomography is superior to computed tomography scanning for response-assessment after radical radiotherapy or chemoradiotherapy in patients with non-small cell lung cancer. J Clin Oncol 2003;21:1285–1292. [PubMed: 12663716]
25. Mohan R, Barest G, Brewster LJ, et al. A comprehensive three-dimensional radiation treatment planning system. Int J Radiat Oncol Biol Phys 1988;15:481–495. [PubMed: 3403328]
26. Burman C, Chui CS, Kutcher G, et al. Planning, delivery and quality assurance of intensity-modulated radiotherapy using dynamic multileaf collimator: A strategy for large-scale implementation for the treatment of carcinoma of the prostate. Int J Radiat Oncol Biol Phys 1997;39:863–873. [PubMed: 9369136]
27. Spirou SV, Chui CS. A gradient inverse planning algorithm with dose–volume constraints. Med Phys 1998;25:321–333. [PubMed: 9547499]
28. Chui CS, LoSasso T, Spirou S, et al. Dose calculation for photon beams with intensity modulation generated by dynamic jaw or multileaf collimations. Med Phys 1994;21:1237–1244. [PubMed: 7799865]
29. Hicks RJ, MacManus MP, Matthews JP, et al. Early FDG-PET imaging after radical radiotherapy for non–small-cell lung cancer: Inflammatory changes in normal tissue correlate with tumor response and do not confound therapeutic response evaluation. Int J Radiat Oncol Biol Phys 2004;60:412–418. [PubMed: 15380574]
30. Kaplan EL, Meier P. Nonparametric estimation from incomplete observations. J Am Stat Assoc 1958;53:457–481.
31. Lardinois D, Weder W, Hany TF, et al. Staging of non–small-cell lung cancer with integrated positron-emission tomography and computed tomography. N Engl J Med 2003;348:2500–2507. [PubMed: 12815135]
32. Munley MT, Marks LB, Scarfone C, et al. Multimodality nuclear medicine imaging in three-dimensional radiation treatment planning for lung cancer: Challenges and prospects. Lung Cancer 1999;23:105–114. [PubMed: 10217614]
33. De Wever W, Meylaerts L, De Ceuninck L, et al. Additional value of integrated PET-CT in the detection and characterization of lung metastases: Correlation with CT alone and PET alone. Eur Radiol 2007;17:467–473. [PubMed: 17180333]
34. Senan S, De RD, Giraud P, et al. Literature-based recommendations for treatment planning and execution in high-dose radiotherapy for lung cancer. Radiother Oncol 2004;71:139–146. [PubMed: 15110446]
35. Vanuytsel LJ, Vansteenkiste JF, Stroobants SG, et al. The impact of (18)F-fluoro-2-deoxy-D-glucose positron emission tomography (FDG-PET) lymph node staging on the radiation treatment volumes in patients with non-small cell lung cancer. Radiother Oncol 2000;55:317–324. [PubMed: 10869746]

36. Van Der Wel A, Nijsten S, Hochstenbag M, et al. Increased therapeutic ratio by ^{18}FDG-PET CT planning in patients with clinical CT stage N2-N3M0 non–small-cell lung cancer: A modeling study. Int J Radiat Oncol Biol Phys 2005;61:649–655. [PubMed: 15708242]

37. Liu HH, Wang X, Dong L, et al. Feasibility of sparing lung and other thoracic structures with intensity-modulated radiotherapy for non–small-cell lung cancer. Int J Radiat Oncol Biol Phys 2004;58:1268–1279. [PubMed: 15001272]

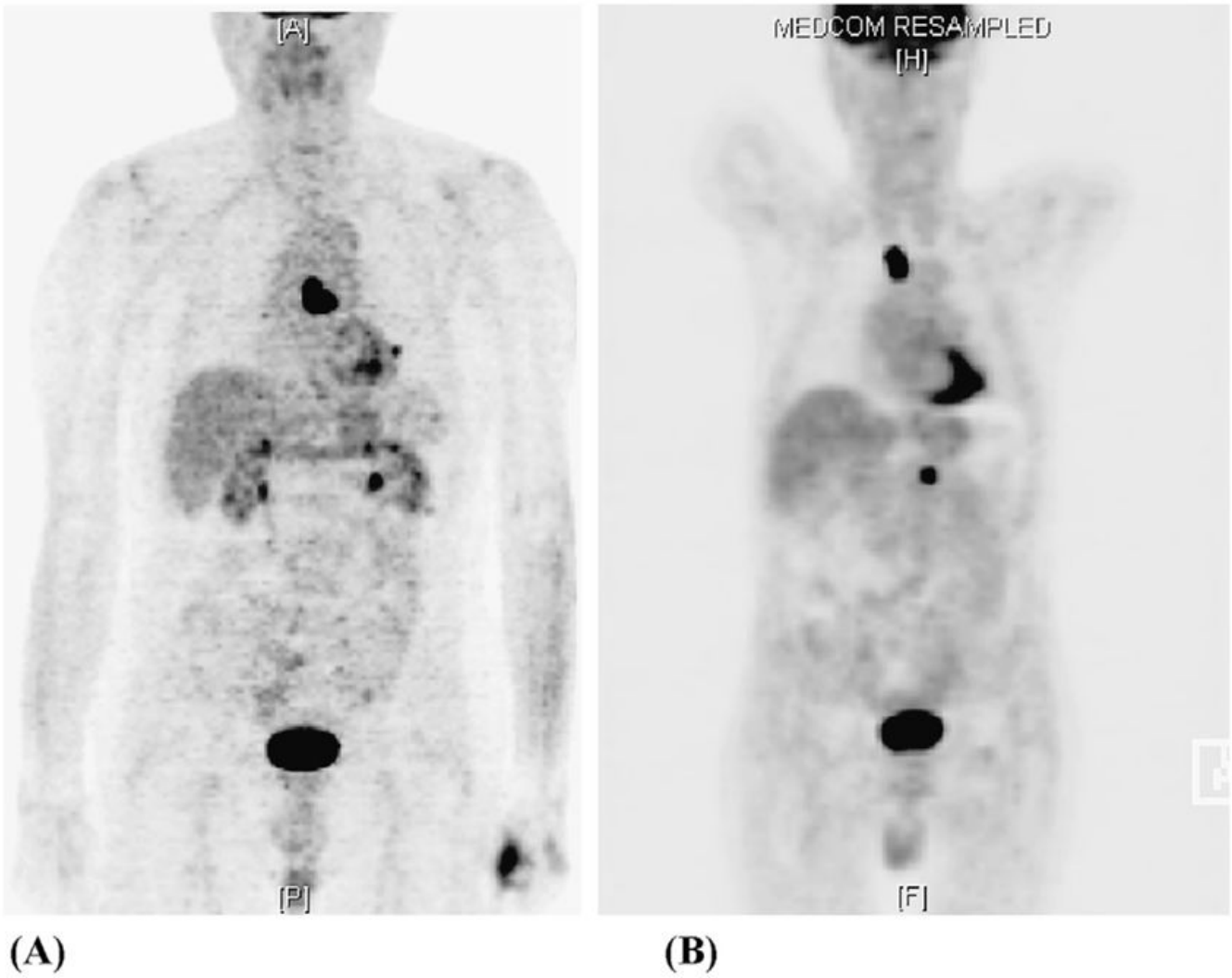

Fig. 1.
Pre-radiotherapy and post-radiotherapy (RT) positron emission tomography (PET) scans for patient with non–small-cell lung cancer (NSCLC). (A) Pre-RT PET scan used for visual incorporation into treatment plan showing centrally located mediastinal uptake. (B) Post-RT PET scan showing recurrence in upper mediastinum outside planning target volume.

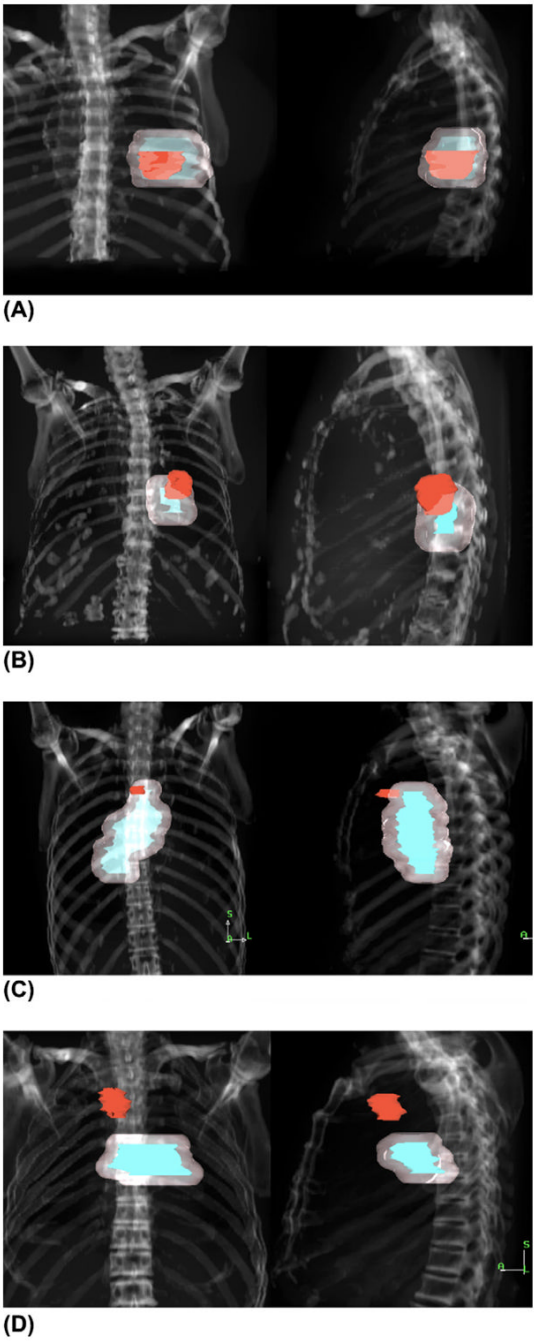

Fig. 2.

Anteroposterior and lateral digitally reconstructed radiographs depicting four patterns of failure: (A) within gross tumor volume (GTV)/planning target volume (PTV); (B) within GTV/PTV and extending outward; (C) within PTV but not GTV and extending outward (marginal miss); and (D) outside PTV (geographic miss). Red indicates recurrence; blue, GTV; and pink, PTV.

Table 1

Patient characteristics (n = 26)

Characteristic	Value
Age (y)	
Median	69
Range	56–86
Gender (*n*)	
Male	10 (38)
Female	16 (62)
Histologic subtype (*n*)	
Adenocarcinoma	9 (35)
Squamous cell cancer	10 (39)
NSCLC, NOS	7 (27)
Stage (*n*)	
I–II	12 (46)
IIIA	6 (23)
IIIB	8 (31)
Recurrent	2 (8)
Restaged IIIA–IIIB	1 (50)
KPS (%)	
Median	80
Range	60–90
GTV (cm^3)	
Median	89
Range	4–397
PTV (cm^3)	
Median	342
Range	66–1,001
Dose (Gy)	
Median	72
Range	50–90

Abbreviations: NSCLC = non–small-cell lung cancer; NOS = not otherwise specified; KPS = Karnofsky performance status; GTV = gross tumor volume; PTV = planning target volume.

Data in parentheses are percentages.

Table 2

Local failure patterns defined by post-RT PET in NSCLC patients treated with definitive RT

	Local failure pattern			
Lesions	**Within GTV/PTV**	**Within GTV/PTV and outward**	**Marginal miss (within PTV and outward)**	**Geographic miss (outside but within 1 cm of PTV)**
Overall (*n* = 34)	13 (38)	15 (44)	4 (12)	2 (6)
Primary (*n* = 26)	12 (46)	13 (50)	1 (4)	0 (0)
Nodal (*n* = 8)	1 (12)	2 (25)	3 (38)	2 (25)

Abbreviations: RT = radiotherapy; other abbreviations as in Table 1.

Data presented as number of lesions, with percentages in parentheses.

Table 3

Dose received by 95% of target volume vs. prescription dose and local failure patterns in primary recurrences stratified by dose >60 Gy vs. <60 Gy

	Local failure pattern (*n* = 26)			
Dose	**Within GTV/PTV**	**Within GTV/PTV and outward**	**Marginal miss (within PTV and outward)**	**Geographic miss (outside but within 1 cm of PTV)**
D_{95} <60 Gy	6	2	0	0
D_{prescr} <60 Gy	6	2	0	0
D_{95} ≥60 Gy	6	11	1	0
D_{prescr} ≥60 Gy	6	11	1	0

Abbreviations: D_{95} = dose received by 95% of target volume; D_{prescr} = dose prescribed to 95% of target volume; other abbreviations as in Table 1.

Int J Radiat Oncol Biol Phys. Author manuscript; available in PMC 2010 July 8.